Gravity Waves at the Interface between Miscible Fluids and at the Top of a Settling Suspension

Georges Gauthier, Jérôme Martin, and Dominique Salin

Laboratoire Fluides Automatique et Systèmes Thermiques Bâtiment 502, Campus universitaire d'Orsay, F 91405 Orsay CEDEX, France

(Received 25 June 2004; published 23 May 2005)

Gravity waves were generated at the interface between miscible fluids, or at the top of a settling suspension or a fluidized bed. For these three systems the dispersion relation was measured and compared to the theory and calculated between two buoyant viscous fluids without surface tension. The experimental findings are found to be in good agreement with theory when effective viscosity and volume-averaged density values are used.

DOI: 10.1103/PhysRevLett.94.204501 PACS numbers: 47.15.Pn, 47.35.+i

Suspensions are ubiquitous in physics and engineering. Colloidal hard-sphere suspensions have been used as model fluids, addressing a variety of statistical physics issues (e.g., the nucleation of a solid phase [1]). On the other hand, the suspension of macroscopic spheres is often represented using an effective fluid description. This approach has been demonstrated convincingly in suspensions of neutrally buoyant particles [2,3]. However, its extrapolation to the nonbuoyant case of sedimenting systems (where fluid and particles differ in density) presents two main difficulties. First, the relative velocity between particles and fluid may affect the configuration of the particle ensemble, and, consequently, the rheological bulk behavior. Second, as the particles settle, regions of pure fluid form, requiring the use of two fluid phases to describe the bulk of the suspension and the behavior of the pseudointerface at the top of the settling suspension, have to be analyzed. Fluid interfaces of this type are not supposed to be stabilized in the macroscopic domain (range of medium to large wavelengths) by effective surface tension effects. Their characterization requires an understanding of their response to external forces, such as buoyancy. The evolution of gravitationally unstable interfaces (e.g., in a Rayleigh-Taylor instability, where a heavy fluid displaces from the top a lighter one [4]) has been studied at great length and in a wide variety of physical contexts: between miscible fluids [5,6], between reactive fluids [7,8], and between a sedimenting suspension and a fluid [9–12]. From an experimental point of view, however, these studies have been hampered by the difficulty of obtaining an initially well-defined ''interface.'' The usual procedure is to turn a cell upside down, where a gravity-stable interface has been created first. The influence of such a rotation on the initial interface remains unclear, however. Instead, the understanding of interface behavior is also possible by studying the response of the pseudointerface to gravitational forces in the stable configuration. This is reported in this Letter. At least in the linear regime, the information obtained from the stable configuration can be theoretically extrapolated to the unstable case, as the two configurations differ only by the sign of the buoyancy term.

We analyze experimentally and theoretically gravity waves propagating at an interface separating two fluids. Experiments are conducted for the following configurations: between two miscible fluids of different densities and viscosities, between the clear fluid and the sedimenting suspension of non-Brownian particles, and at the top of a fluidized bed. The latter two configurations are obtained by conducting a sedimentation experiment leading to a settling front, in the first case, and by controlling the upward liquid flow rate (which compensates for the sedimentation velocity [13] and leads to a stationary top front), in the second case. In the fluidization experiments, the flow rate also controls the volume fraction of the suspended particles, with larger flow rates leading to smaller volume fractions. In all experiments, the dispersion relation corresponding to the gravitational waves is obtained by measuring the response of the interface to an imposed perturbation of controlled amplitude and frequency. We find that the resulting dispersion relation is identical for the sedimentation and fluidization experiments, for all volume fractions and particle sizes considered. A theoretical dispersion relation is then derived, corresponding to gravity waves between two buoyant miscible and viscous fluids. The measured dispersion relation for the three experiments is found to be in good agreement with the theoretical one, when, in the case of suspensions, effective viscosity and averaged density values are used. The agreement applies to

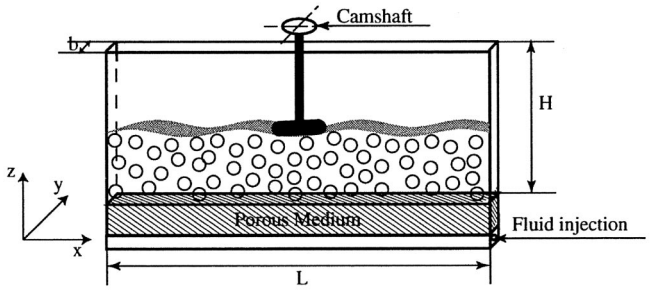

FIG. 1. Sketch of the experimental setup. $L = 50$ cm, $H = 42$ cm, and $b = 5$ mm.

the macroscopic behavior probed, in the range of medium and large wavelengths, and may not necessarily apply to short-wave perturbations, where effective surface tension effects are of equal importance.

The experimental setup is sketched in Fig. 1. The Hele-Shaw cell is open at the top and consists of two parallel glass plates of size 50 cm $\times$ 50 cm, separated by a small gap $b = 5$ mm. The cell was chosen sufficiently large to avoid reflection at the lateral boundaries. A thin porous medium was placed at the bottom inlet of the cell, to ensure a uniform velocity in the fluidization experiments. The suspended particles are glass beads of diameter $d \in [100, 125]$ μm and relative density 2.5. Experiments were performed with volume fractions in the range $\Phi \in [0.30, 0.52]$, corresponding to upward flow velocities between 0.3 and 1.95 mm/s. These small velocities ensure a small particle Reynolds number ($\mathrm{Re}_p = U_{\mathrm{fluid}} d/\nu_{\mathrm{fluid}} \approx 0.1$) and, hence, laminar flow and a stable fluidized bed. Interface perturbations were generated by a vertically oscillating cylindrical hammer 1.5 cm long and 4 mm in diameter, the end of which was placed at the interface. The oscillatory motion was implemented through a camshaft rotated by a stepping motor. We varied the frequency f in the range $[0.5, 5]$ Hz and kept the amplitude equal to 0.5 cm. The initial interface was stationary in the fluidization experiments, and settled at a constant velocity in the sedimentation ones. The results were captured on a video camera (IIDC CMOS) and analyzed with Image J software. In the sedimentation experiments, the perturbation device and the video camera were fixed on a glide, translated by a dc motor, with the same velocity as the sedimenting front. The experiments between two miscible fluids consisted of a mixture of water, glycerol, and salt ($\rho = 1260$ kg/m^3 and $\eta = 8 \times 10^{-3}$ Pa s) for the underlying heavier fluid and of pure water for the overlying lighter one. In these experiments, the frequency f of the imposed perturbation was in the range $[0.5, 1.25]$ Hz.

Figure 2 is a snapshot of the interface response for a fluidized bed: small-amplitude waves propagate outwards from the initial perturbation and are damped at a short distance away. Such waves were observed in the frequency range $[1.25, 3.5]$ Hz. At higher frequencies, the waves were overdamped, whereas at lower frequencies, the amplitude of the perturbation was not detectable (the forcing mechanism becomes inefficient at low frequencies).

A spatiotemporal diagram of the results corresponding to Fig. 2 is shown in Fig. 3. The white strips in the figure correspond to the traveling waves; they are parallel equidistant straight lines, showing that the waves are periodic and have a constant velocity. A Fourier transform showed that the waves have the frequency of the imposed perturbation and do not contain any harmonics, which should allow comparison with a linear theory. The inset of Fig. 3 displays a typical snapshot of the height of the interface. Such a curve was fitted by a sinusoidal form with a decaying amplitude. The so-obtained damping length is very short and comparable with the wavelength λ. For each frequency, 2048 images were processed, and the resulting values (which differ typically by ± 10 m^{-1} for the real part of the wave number) were averaged.

Fluidized beds are often used to provide stationary suspensions in the laboratory frame. However, fluidized and sedimenting suspensions are not necessarily equivalent, as the volume-averaged velocity of the two phases is zero in sedimentation, while it is equal to the upward flow velocity in fluidization. This difference may have two effects. First, the fluidization velocity may impart an inertial contribution to the suspension. Second, the nonzero velocity profile across the gap of the cell, in the fluidized bed case, may lead to a different particle configuration (concentration profile) in the gap, which could affect the dynamic response of the suspension. We investigated these possible effects by performing experiments at different particle volume fractions, Φ, and perturbation frequencies, in both sedimentation and fluidization configurations. The results, plotted, respectively, as open and plain symbols in Fig. 4, compare very well. These trends support the contention that neither the mean flow rate nor the configuration in the gap influence wave propagation. The latter assertion was also tested by changing the bead size, which may affect the concentration variation in the gap [14,15]. Experiments carried out with larger beads

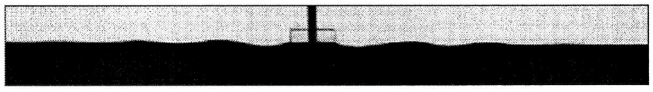

FIG. 2. Snapshot of the waves generated at the top of a fluidized bed. The volume fraction is $\Phi \approx 0.37$, the suspending fluid is water, and the beads are 125 μm in diameter. (Window width: 22 cm of the 50 cm wide Hele-Shaw cell.)

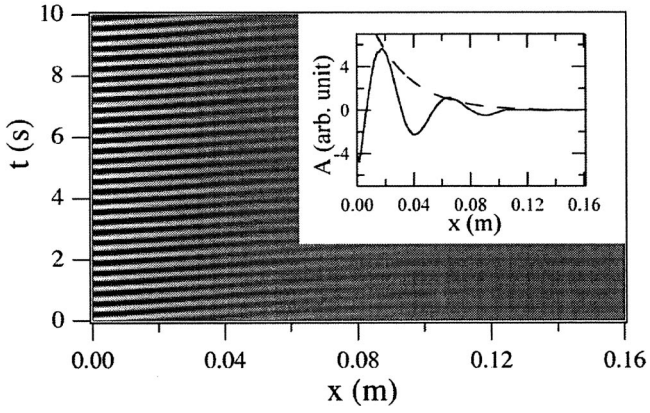

FIG. 3. Spatiotemporal image of the interface amplitude corresponding to Fig. 2. Imposed frequency: 3 Hz; amplitude: 0.5 cm. Inset: Interface height and exponential fit of its amplitude.

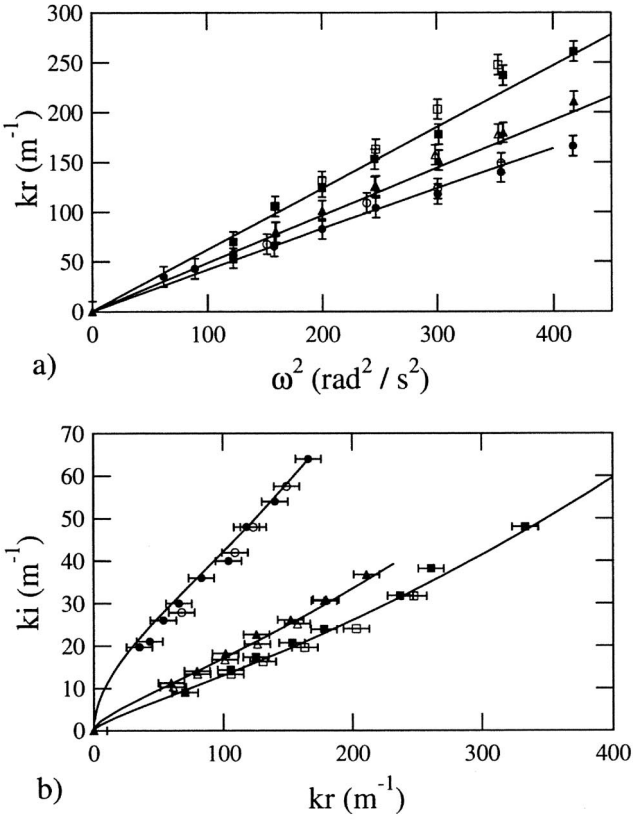

FIG. 4. Dispersion relations for gravity waves in sedimentation and fluidization. (a) Wave number k_r versus ω^2 ($\omega = 2\pi f$). (b) Damping rate k_i versus k_r. Measurements at the interface between the clear fluid and the fluidized or sedimenting suspension (plain or open symbols, respectively). Solid lines: theoretical predictions. (●, ○) $\Phi = 0.52$; (▲, △) $\Phi = 0.44$; and (■, □) $\Phi = 0.30$.

($d \in [200, 250]$ μm) did not show any significant effect on the dispersion curve.

Suspensions are often described as a homogeneous effective fluid with a volume-averaged effective density, $\rho_{\text{susp}} = \rho_{\text{solid}}\Phi + \rho_{\text{fluid}}(1 - \Phi)$ and an effective viscosity $\eta_{\text{susp}} = \eta_{\text{fluid}}\eta_r(\Phi)$, where the relative viscosity $\eta_r(\Phi)$ depends only on the volume fraction Φ [16–18]. With this model, when the wavelength is large compared to the thickness of the cell, the perturbation in the flow velocity is $\vec{\tilde{v}} = [\tilde{u}(x, z, t)\vec{e}_x + \tilde{w}(x, z, t)\vec{e}_z] \times h(y)$, where, in this limit of low frequencies, $h(y)$ is the Poiseuille (parabolic) profile. However, because the viscous length $\delta = \sqrt{2\nu/\omega}$ ($\nu = \eta/\rho$ and $\omega = 2\pi f$) is smaller than the gap b in our experiments (e.g., $\delta \approx 1$ mm for $\Phi = 0.4$ and $f = 1$ Hz), the phase of the velocity will vary across the gap and $h(y) = \frac{1}{N}(1 - \frac{\cos(\xi y)}{\cos(\xi b/2)})$, where $\xi = (1 + i)\delta$ and N is the normalization coefficient. In the long-wave approximation, the gap-averaged velocity $\vec{v} = (1/b)\int_{-b/2}^{b/2} \vec{\tilde{v}} dy$, obeys continuity ($\text{div}\,\vec{v} = 0$) and the Stokes-Darcy equation [6,19],

$$\rho \frac{\partial \vec{v}}{\partial t} = -\vec{\nabla}P + \eta\Delta\vec{v} - (\eta/K_{\text{eff}})\vec{v} + \vec{g}\delta\rho,$$

where $K_{\text{eff}} = b^2[\frac{2}{\xi b}\tan(\xi b/2) - 1]/[2\xi b \tan(\xi b/2)]$ is the effective permeability. The above equations also hold in the case of fluidization, as the Strouhal number $\text{St} = \omega/U_f k$, which is the ratio of the phase velocity to the fluidization velocity, is large, and the inertial term $\rho(\vec{U}_f \cdot \vec{\nabla})\vec{v}$ is negligible.

Writing the z component of the velocity perturbation as $w(x, z, t) = W(z)e^{i(kx-\omega t)}$, with k complex and ω real, and assuming the same form for the x component u and the pressure, one finds after linearization, the following equation:

$$[i\omega + \nu(D^2 - q^2)](D^2 - k^2)w = 0$$

with $D = d/dz$ and $q^2 = -(i\omega/\nu) + k^2 - K_{\text{eff}}^{-1}$. This equation is satisfied in each of the two fluids. Its solution in a semi-infinite domain is $w = Ae^{\pm kz} + Be^{\pm qz}$, where the appropriate sign is chosen in each fluid region to ensure exponential decay away from the sharp interface. Continuity in the two velocity components, the tangential viscous stress and the pressure at the interface, leads to a set of four homogenous linear equations. The dispersion relation is obtained by setting the determinant to zero. This must be computed numerically. We, first, tested the validity of the so-obtained dispersion relation of gravitational waves between two nonmixing miscible fluids, by performing an experiment with two real fluids. The dispersion curves, for $f \in [0.5, 1.25]$ Hz, are displayed in Fig. 5, together with the corresponding theoretical predictions. The good agreement between the two validates the theoretical description. Noteworthy is the fact that in the range of frequencies studied, effects of surface tension [20] act at smaller wavelengths and cannot be accessed in the range of frequencies we used.

Applying the above theory to suspensions requires the value of the effective relative viscosity function $\eta_r(\Phi)$. This was determined by a best fit with the experimental data. The corresponding dispersion curves for the three different volume fractions are shown in Fig. 4. A good agreement is observed between theory and experiments for all cases tested in sedimentation and fluidization. The relative viscosities used were $\eta_r = 33 \pm 3$, $\eta_r = 9.25 \pm 1.25$, and $\eta_r = 3 \pm 0.5$ for $\Phi = 0.52$, $\Phi = 0.44$, and $\Phi = 0.3$, respectively. These values can be compared to expressions commonly found in the literature. For example, one can cite the empirical law of Krieger [18] $\eta_r = (1 - \Phi/\Phi_m)^{-1.82}$ (proposed for small volume fractions, but also used at finite values) and the expression by Ball and Richmond [16] $\eta_r = (1 - \Phi/\Phi_m)^{-3/2}$ and by Mills [17] $\eta_r = (1 - \Phi)/(1 - \Phi/\Phi_m)^2$. A key parameter in these expressions is the packing volume fraction Φ_m (at

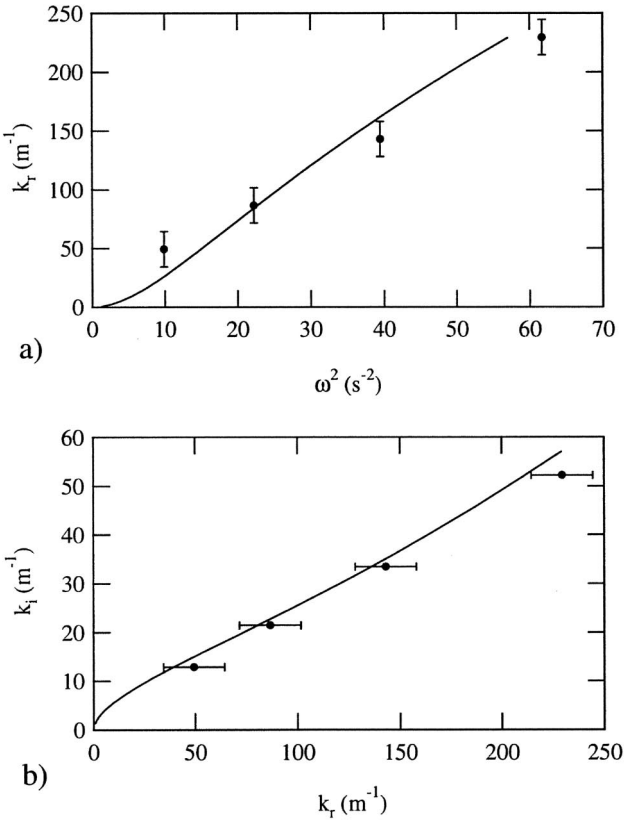

FIG. 5. The dispersion relation of gravity waves between two miscible fluids. (a) Wave number k_r versus the square of the wave frequency ω^2. (b) Damping rate k_i versus wave number k_r. Symbols: experimental results; solid lines: theoretical predictions.

which the effective viscosity becomes infinitely large). Currently, there is no consensus on its value. If we use the measured value in the sediment, $\Phi_m = 0.58$, the comparison between the best-fit parameters and the above three models for the effective viscosity is good for $\Phi = 0.3$ and 0.44. However, the three expressions disagree with each other at the largest value $\Phi = 0.52$, where $\eta_{r,\mathrm{Krieger}} = 62$, $\eta_{r,\mathrm{Ball}} = 30$, and $\eta_{r,\mathrm{Mills}} = 34$ to be compared to our experimental value $\eta_r = 33 \pm 3$. Note that the latter shows that the Krieger expression should not be used at high concentrations.

In this Letter, we conducted experiments of gravity waves on the interface between a clear fluid and a sedimenting suspension, or between a clear fluid and a fluidized suspension. The experimental configuration corresponds to a stable interface. For comparison, waves at the interface between two miscible fluids were also studied. For suspensions of different volume fractions and particle sizes, we obtained an identical response of the interface in both sedimentation and fluidization. The corresponding dispersion relations were measured for the three systems. Our measurements agree with the theory of gravity waves between two buoyant and viscous fluids, with an effective viscosity and averaged density for suspensions. This demonstrates that the same description can be applied to the unstable case.

We acknowledge fruitful discussions with Professor E. J. Hinch and Professor Y. C. Yortsos. We thank Dr. A. Daerr for providing Firewire Image J plug-ins, S. Girard, and N. Verdon for helping with the experiments, and G. Chauvin and R. Pidoux for building the experimental setup.

[1] J. L. Harland, S. I. Henderson, S. M. Underwood, and W. van Megen, Phys. Rev. Lett. **75**, 3572 (1995).
[2] P. R. Nott and J. F. Brady, J. Fluid Mech. **275**, 157 (1994).
[3] C. J. Koh, P. Hookham, and L. G. Leal, J. Fluid Mech. **266**, 1 (1994).
[4] S. Chandrasekhar, *Hydrodynamic and Hydromagnetic Stability* (Oxford University Press, New York, 1961), and references therein.
[5] J. Fernandez, P. Kurowsky, P. Petitjean, and E. Meiburg, J. Fluid Mech. **451**, 239 (2002).
[6] J. Martin, N. Rakotomalala, and D. Salin, Phys. Fluids **14**, 902 (2002).
[7] M. Böckmann and S. C. Müller, Phys. Rev. Lett. **85**, 2506 (2000).
[8] J. Martin, N. Rakotomalala, D. Salin, and M. Böckmann, Phys. Rev. E **65**, 051605 (2002).
[9] A. K. Didwania and G. K. Homsy, *I & EC Fundamentals* 20, 318 (1981).
[10] T. Loimer and U. Schaflinger, Phys. Fluids **10**, 2737 (1998).
[11] C. Völtz, W. Pesch, and I. Rehberg, Phys. Rev. E **65**, 011404 (2002).
[12] T. W. Pan, D. D. Joseph, and R. Glowinski, J. Fluid Mech. **434**, 23 (2001).
[13] J. Martin, N. Rakotomalala, and D. Salin, Phys. Rev. Lett. **74**, 1347 (1995).
[14] F. Rouyer, J. Martin, and D. Salin, in *Proceedings of the 20th IUPAP International Conference on Statistical Physics* (UNESCO and Sorbonne, Paris, 1998).
[15] D. Bruneau, F. Feuillebois, J. Blawzdziewicz, R. Anthore, and J. Hinch, Phys. Fluids **8**, 2236 (1996); D. Bruneau, F. Feuillebois, J. Blawzdziewicz, and R. Anthore, Phys. Fluids **10**, 55 (1998).
[16] R. C. Ball and P. Richmond, Phys. Chem. Liq. **9**, 99 (1980).
[17] P. Mills, J. Phys. (Paris), Lett. **46**, 301 (1985).
[18] I. M. Krieger, Adv. Colloid Interface Sci. **3**, 111 (1972).
[19] P. Gondret and M. Rabaud, Phys. Fluids **9**, 3267 (1997).
[20] P. Petitjeans, P. Kurowski, J. Fernandez, and M. Hoyos, J. Chim. Phys. Phys.-Chim. Biol. **96**, 991 (1999).